Efficient gene targeting and foreign DNA removal by homologous recombination in the picoeukaryote *Ostreococcus*

Jean-Claude Lozano[1,2,†], Philippe Schatt[1,2,†], Hugo Botebol[1,2], Valérie Vergé[1,3], Emmanuel Lesuisse[4], Stéphane Blain[1,2], Isabelle A. Carré[5] and François-Yves Bouget[1,2,§]

1-Université Pierre et Marie Curie (Paris 06), Observatoire Océanologique, F-66651, Banyuls/Mer, France.

2-Centre National de la Recherche Scientifique, Unité Mixte de Recherche, UMR7621, LOMIC, Laboratoire d'Océanographie Microbienne, F-66651, Banyuls/mer, France.

3-Centre National de la Recherche Scientifique, Unité Mixte de Service, UMS2348,F-66651, Banyuls/Mer, France.

4-Lab Mitochondria Metals and Oxidative Stress, Institut Jacques Monod, CNRS-Université Paris Diderot, France.

5- School of Life Sciences, University of Warwick, Coventry, U.K.

† Equal contribution

§ -Corresponding author

E-mail: fy.bouget@obs-banyuls.fr

Running title: Gene targeting in *Ostreococcus*

Summary

With less than 8000 genes and a minimalist cellular organization, the green picoalga *Ostreococcus tauri* is one of the simplest photosynthetic eukaryote. *O. tauri* contains many plant-specific genes but exhibits a much lower gene redundancy. The haploid genome is extremely dense with few repeated sequences and rare transposons. Thanks to the implementation of genetic transformation and vectors for inducible overexpression/knockdown this picoeukaryotic alga has emerged in recent years as a new model organism for functional genomics analyses and systems biology. Here we report the development of an efficient gene targeting technique, which we use to knock out the *nitrate reductase* and *ferritin* genes and to knock-in a luciferase reporter in frame to the ferritin native protein. Furthermore, we show that the frequency of insertion by homologous recombination was greatly enhanced when the transgene was designed to replace an existing genomic insertion. We propose that a natural mechanism based on homologous recombination may operate to remove foreign DNA sequences from the genome.

Abbreviations:
HR: Homologous recombination; RI, random insertion; *NR*, Nitrate reductase

INTRODUCTION

Over the past twenty years the extensive development of genetic transformation technologies in model organisms has revealed different mechanisms of transgene integration. Gene targeting by homologous recombination (HR) is the method of choice either to delete a gene or to introduce a selected mutation or a fuse a tag to a protein. In bacteria and in a few eukaryotic model organisms such as the yeast *Saccharomyces cerevisiae*, HR occurs preferentially over random integration of homologous sequences, however for most eukaryotes, transgene integration occurs almost exclusively in a random fashion.

Random insertion of transgenes and targeted insertion by homologous recombination are based on distinct mechanisms of DNA repair. Random insertion is based on non-homologous end joining (NHEJ) repair of double-strand breaks (DSBs) in DNA (Heyer et al., 2010). Targeted insertion is mediated by the Rad51 recombinase, which catalyzes DNA strand exchange between damaged DNA and intact, homologous DNA sequences (Shinohara et al., 1992). This mechanism is conserved between bacteria and eukaryotes (Heyer et al., 2010). The Spo11 protein mediates an additional mechanism of homologous recombination specific to eukaryotes, which allows formation of crossovers between homologous chromosomes pairs at meiosis to ensure their proper segregation (Keeney et al., 1997). This is of crucial importance to allow exchanges of DNA between homologous chromosomes and the shuffling of genetic information.

Gene targeting by homologous recombination remains difficult in most photosynthetic eukaryotes, with the exception of mosses (Schaefer and Zryd, 1997). Most attempts to knock out genes by HR in algae and in higher plants were designed to disrupt the *Nitrate reductase* gene (*NR*). This strategy greatly simplified the identification of homologous recombination events, as knock-out mutants grew on ammonium but failed to grow in the presence of nitrate. Gene knock out by HR in algae was first reported 20 years ago in the Chlorophyta *Chlamydomonas*, but gene targeting by HR remains very difficult in this model organism (Sodeinde and Kindle, 1993; Zorin et al., 2009). In contrast, efficient gene targeting has been reported for two unicellular algae: the thermophilic acidophil red alga *Cyanidioschizon merolae* and the Heterokontophyta *Nannochloropsis sp*. (Minoda et al., 2004; Kilian et al., 2011).

Ostreococcus tauri (Prasinophyceae) has recently emerged as new marine model organism. This tiny unicellular alga has a minimalist organization that allows approaches such as whole cell imaging by electron cryotomography (Gan et al., 2011). Its haploid genome is compact and gene-dense, with very little gene redundancy (Derelle et al., 2006). Functional genetic analyses in this organism are facilitated by an efficient genetic transformation protocol. This enabled for example the study of phenotypes caused by constitutive or inducible overexpression or knockdown of gene expression, or the monitoring of gene activity by *in vivo* imaging of luciferase reporter constructs (Corellou et al., 2009; Moulager et al., 2010; Djouani-Tahri et al., 2011b). These tools were used in our research to analyze the genetic circuits and light signaling pathways to the circadian clock (Monnier et al., 2010; Djouani-Tahri et al., 2011a; Heijde et al., 2010; Pfeuty et al., 2012), and to demonstrate the presence of a novel type of non-transcriptional circadian clock shared with human red blood cells (O'Neill et al., 2011).

However, antisense silencing of gene expression proved difficult in *O. tauri.* In our experience, phenotypes were not always correlated to reduced transcript levels. RNA-interference (RNAi) approaches are unlikely to be successful because *O. tauri* lacks key components of the RNA-induced-silencing complex, such as Dicer and Argonaute. However, homologues of Rad51 and Spo11 were identified in this organism, suggesting the presence of HR mechanisms involved in DSB break repair and meiosis (Derelle et al., 2006). This suggested that targeted gene disruption by HR might be achievable.

In this paper, we describe a method for efficient transgene insertion by HR This was used to knock out two different genes, *nitrate reductase* (*NR)* and *ferritin,* and in a knock-in experiment to insert a luciferase reporter gene in frame at the *ferritin* locus. Interestingly the frequency of transgene insertion by HR varied between 1 and 100% depending on whether the construct was designed to replace wild-type DNA sequences or to replace an existing transgene insertion. We propose that HR may normally operate in *Ostreococcus* to eliminate foreign DNA sequences from the genome.

RESULTS

Knock-out of the *NR* gene by homologous recombination

O. tauri is normally able to grow on Artificial Seawater (ASW) containing either nitrate or ammonium as the sole source of nitrogen (nitrate-ASW and ammonium-ASW respectively). However loss of nitrate reductase function in *NR knock-out* (NR^{KO}) lines should result in the loss of ability to grow on nitrate-ASW. This provided us with a simple and efficient method to identify homologous recombination events.

O. tauri is haploid and *NR* is encoded by a single gene located on Chromosome 10. We designed a disruption cassette containing about 2 kbp of sequence homologous to the *NR* locus. This was interrupted by the *KanMx* selection marker, which confer resistance to the antibiotic G418. The Kan-Mx marker was inserted either in sense or in antisense orientation relative to the *NR* sequence to produce the *KanMx-s* and *KanMx-as constructs* (Figure 1a). This was used to determine whether the orientation of the *KanMx* gene relative to the *NR* gene affected the frequency of insertion by HR. These constructs were introduced into wild-type (WT) cells using the standard electroporation protocol (Corellou et al., 2009). Transformants were selected on semi-solid ammonium-ASW agarose plates containing 1mg/ml G418. G418-resistant transformants were then tested for their ability to grow in nitrate-ASW. Clones that grew under these conditions identified putative homologous recombination events (Figure 1b).

One G418-resistant *KanMx-s* transformant out of 107, and 8 G418-resistant *KanMx-as* transformants out of 425 grew in nitrate-ASW. PCR analyses were carried out to confirm the mechanism of transgene insertion in these putative HR lines (Figure 2, Table 1). The primers F1 and R1 were used to test for the presence of an intact *NR* locus. A 0.6 kbp fragment was amplified from WT cells. The same fragment was amplified from all of the *KanMx-as* transformants that grew in nitrate-ASW, confirming that they were the product of random (RI) in the genome. In contrast this fragment was not amplified from lines that failed to grow in nitrate-ASW, showing that the *NR* gene had been disrupted by insertion of the transgene. This was confirmed by the amplification of a 3 kbp product in all HR lines using a combination of primers F2 in the selection gene and R2 in the *NR* sequence.

Southern blot analyses were carried out to check the number and pattern of transgene insertions in the HR lines. Genomic DNA was digested with *Kpn*I, which cleaved the insertion cassette immediately upstream of the *KanMx* resistance gene (Figure 2a). Hybridization of a *NR* specific probe (P1) revealed a single band around 20 kbp in WT and RI

cells, corresponding to the intact *NR* locus (Figure 2b). In contrast, a 6.5 kbp band was detected in HR lines, indicating the presence of the additional *Kpn*I site resulting from insertion of the *KanMx* gene at the *NR* locus. No additional band was detected indicating that no additional insertions had occurred in the HR lines. A similar, 6.5 kbp band was detected in HR lines using a probe specific to the *KanMx* transgene (P2) whereas a 15 kbp band was observed in the single RI line tested, corresponding to a random insertion of the transgene.

Similar experiments were performed in the lines resulting from the *KanMx-s* transformation (Figure S1). PCR products were obtained at the expected size for HR, i.e. 3.2 kbp and 2.2 kbp using (F3, R2) and (F1, R1) primer couples respectively. Hybridization of genomic DNA digested with *Kpn*I to the *NR* P1 probe revealed a band at a size (4.9 kbp) consistent with HR of the *KanMx-s* construct at the *NR* locus (Figure S1).

In summary, the molecular characterization of HR events at the *NR* locus indicated that HR occurred at frequency around 1-2%, regardless of orientation of the antibiotic resistance cassette (Table 1). No additional insertion took place through a random process in any of the HR lines analysed. The first generation of *KanMx-as* and *KanMx-s* HR lines were denoted HR1 *KanMx-as* and HR1 *KanMx-s*, respectively. The nomenclature used to describe these lines and the lineages of subsequent HR lines are summarized in Figure 1c.

Complementation of the NR mutation by HR occurs at a very high frequency

In order to confirm that the lack of growth on nitrate-ASW was due to the disruption of the *NR* gene, we tested whether replacement of the disrupted copy of the *NR* gene in *HR1* lines with the wild-type sequence restored a wild-type phenotype. One *HR1KanMx-s* line and one *HR1KanMx-as* line were transformed with a 4.2 kbp *Nit* fragment comprising the full *NR* gene (see Figure 1). Transformants that had acquired a wild-type copy of the *NR* gene were selected on nitrate-ASW medium. These transformants (denoted *HR2NitKanMx-s* /*HR2NitKanMx-as* depending on the parental HR1 *KanMx-s* or *KanMx-as* lines) were expected to arise either from replacement by HR of the disrupted copy of the *NR* gene, or by random insertion of the *Nit* fragment elsewhere in the genome. The latter scenario should result in retention of the *KanMx* cassette at the *NR* locus and therefore resistance to the antibiotic G418. Surprisingly none of the *HR2NitKanMx-s* and *HR2NitKanMx-as* transformants (n=54 and 219, respectively) grew in the presence of G418 (Table 2). This suggested that the native *NR* locus had been restored in all of these transformants, by

homologous recombination. This was confirmed by PCR and southern blot analyses as above (Figure 3)

HR frequency is increased at loci containing foreign DNA

The very high frequency of homologous recombination in the complementation experiment contrasted with that of the original transformation experiments (100% as compared to 1-2%). We first hypothesized that the frequency of HR might be affected by the different types of selection used in these experiments. In order to test this hypothesis, we generated *HR1Nat* lines that contained a *Nat1* insertion at the *NR* locus (see Figure S2). The *KanMx* and *Nat1* selection cassettes share the *histone H4* promoter and *Tef* terminator sequences (0.4 and 0.25 kbp long respectively). We therefore transformed the *pH4:Nat1* construct into the *HR1KanMx-s* line in order to target the selection cassette (Figure S2a). Four out of 122 transformants showed a phenotype expected from HR, i.e. resistance to CloNat and sensitivity to G418 (Table 2). These were designated *HR1Nat* (Figure 1c). PCR analysis using *PH4* and *Tef* specific primers confirmed that the *KanMx* marker had been replaced by *Nat1* in these lines. We were also able to replace the *Nat* selection cassette with *KanMx* in a subsequent experiment (Figure S2b). Transformation of a *HR1Nat* line using the *KanMx-s* construct to replace the *Nat1* resistance gene in *HR1Nat* line resulted in 39 transformants out of 60 becoming sensitive to CloNat (Table2). The loss of the *Nat1* marker in these lines suggested that they were the product of homologous recombination, and this was confirmed in PCR analyses (Figure S2). The frequency of HR in this experiment was comparable to that to those obtained using the *Nit* construct in the complementation experiment above (approximately 65%). As the acquisition of the *KanMx-s* and the *Nit* sequences are selected for using different mechanisms, this showed that the efficiency of HR was unrelated to the selection mechanism. However, the frequency of HR was much greater when transforming the *KanMx*-s construct into *H1RNat* than in wild-type cells (65% as compared to 1-2 %). This suggested that the frequency of HR was linked to the recipient line rather than to the specific construct used in the transformation experiment. We hypothesized that the interruption of the *NR* locus by a foreign sequence may increase the rate of HR, whether to restore the native DNA sequence or to replace one foreign DNA insertion with another. According to this hypothesis, HR frequencies should return to very low levels upon removal of the foreign DNA sequence. Thus, when *HR2Nit* cells (produced by complementation of the *HR1 NR* knock-out lines) were transformed using the *KanMx-s* construct, all of 192 transformants were the product of random insertion rather than HR

(Figure S3, Table 2). These results indicate that HR frequencies are low whether targeting the native or the restored *NR* gene, and are high when targeting a disrupted *NR* locus.

Importance of the length of homologous sequences

Homologous recombination occurred at frequencies ranging between 65 and 100% when targeting the disrupted *NR* locus using the *Nit* and *KanMx-s* constructs, which both contain 2.5 kbp of flanking sequences homologous to *NR*. In contrast the HR frequency was much lower (4%) using the *pH4:Nat1* construct which only comprises 0.25 and 0.5 kbp of sequence homologous to the *KanMx* cassette (Table 2). This raises the hypothesis that the length of homologous sequence may be a critical parameter in the HR efficiency. This possibility was explored by systematically testing the effect of the length of homologous sequences on the efficiency of gene targeting. *HR1Nat* cells were transformed with a *KanMX-s* construct that contained *NR* flanking sequences of various lengths (0.5-2.5 kpb). The HR frequency with the full-length construct was approximately 65% and decreased to 26% and 5% when using 1 and 0.5 kbp-long homologous sequences (Figure 4). This result indicates that a length of homologous sequence greater than 2.5 kbp is required for optimal gene targeting by HR.

Role of chromatin structure

There is evidence that chromatin packing regulates homologous recombination at immunoglobulin loci in *Drosophila* (Cummings et al., 2007). Furthermore, histone acetyl transferase activity was required for homologous recombination in Hela cells, suggesting a role for chromatin structure in this process (Kotian et al., 2011). We therefore hypothesized that the dramatic increase in recombination frequencies upon insertion of the *KanMx* cassette in HR1 lines may be due to remodeling of the local chromatin. This effect would then be reversed upon removal of the *KanMx* cassette, leading to lower recombination rates in complemented, HR2 lines. We tested for changes in nucleosome density at the *NR* locus by quantifying the *in vivo* binding of Histone H3 in chromatin immunoprecipitation (ChIP) experiments. In addition we tested for changes in histone H3 modifications that either open up the chromatin (H3 acetyl K9) or that result in a more compact structure (H3 trimethyl K4). Three different regions were assayed surrounding the insertion site, including the *NR* promoter (Region 1), the 3'end of the *NR* coding region (Region 2), and Region3 which falls out of the homologous sequence used in our *KanMx-s* construct. No consistent reversible

change was observed across any region that would support our hypothesis that one of the specific histone modification tested could regulate the frequency of HR (Figure 5). It remains possible that other types of histone modifications, which were tested as part of these experiments, take place during homologous recombination. Alternatively DNA methylation may be involved.

Knocking-out and tagging of the native *ferritin* gene

Experiments so far had focused on the *NR* locus, which was especially attractive because of the ease with which knock-out mutants can be identified. To determine whether the use of HR-mediated gene targeting could be generalized to other loci in *O. tauri*, we tested its application to the *ferritin* gene which does not have a selectable phenotype.

In *O. tauri* the ferritin is encoded by a single gene that is located on Chr2 (Figure 6). A similar approach as described for *NR* was used to disrupt the *ferritin* gene. WT cells were transformed with the gene interrupted by the *KanMx* selection marker. 96 transformants were obtained after selection on G418 medium. These were subsequently screened by PCR to identify lines resulting from HR events (Figure 6a). 2 HR lines (denoted *HRFe*) were identified by the production of a PCR band at 0.9 kbp using a *KanMx* specific primer (FFt) and a reverse primer located in the *Ferritin* sequence (RFo). In addition, the 0.9 kbp band amplified from WT cells using *ferritin* internal primers (FFe and RFe) was replaced by a band a 2.5 kbp indicating that the *KanMx* sequence had inserted into the endogenous *ferritin* locus. The frequency of recombination (2%) was in the range observed when targeting the WT *NR* gene.

Gene targeting by HR is useful to generate gene knock-outs, but also to knock-in sequences such as epitope tags downstream of protein coding sequences. Translational reporter fusions to the firefly luciferase reporter gene have been extensively used to monitor circadian changes in gene expression in *Ostreococcus* (Corellou et al., 2009; Moulager et al., 2010; Djouani-Tahri et al., 2011b). We designed a knock-in construct to insert the luciferase sequence downstream of, and in frame with, the ferritin coding region. The construct comprised the *luciferase-KanMx* flanked upstream by the *ferritin* coding region (lacking a stop codon) and on the other side by downstream sequences of the *ferritin* gene (Figure 6b). A 1.2 kbp product indicative of HR was amplified from 10 out of 42 transformants using the *KanMx* specific primer FH4 and the external primer RFi (24%). These 10 *HRFlu* lines also failed to yield a product at 0.27 kbp using the *ferritin*-specific primers FFo and RFo, which

was detected in Wt and random insertion lines (Figure 6b). Western blot analysis using an anti-luciferase antibody revealed a protein band at about 85 kda in both *RIFlu* and *HRFLu* lines (Figure 6b), which confirmed the production of a *Ferritin-luc* fusion protein. These results indicate that HR can be used to generate not only knock-out but also knock-in recombinants in *Ostreococcus tauri*.

DISCUSSION

Efficient gene targeting by homologous recombination in Ostreococcus tauri

The ability to target DNA constructs to specific homologous regions of the genome provides a tool for functional genomics analysis that is available only in few eukaryotic model systems and even fewer photosynthetic organisms.

Here, we report the successful targeting of the *nitrate reductase (NR)* locus in *O. tauri*, in more than 10 independent experiments. We further demonstrate the knock-out of a non-selectable gene, *ferritin*, at a similar frequency. Knock-out lines were also obtained for the blue light photoreceptor LOV-HK and will be reported elsewhere (Djouani-Tahri, EB and Bouget FY, personal communication). Southern experiments indicated that no illegitimate integration occurred in HR lines, suggesting that homologous recombination which occurs by double strand break repair and random insertion (which occurs by non-homologous end joining) are mutually exclusive in *O. tauri*. The results of Southern and PCR analyses supported the hypothesis that gene knock out results exclusively from double crossing-over events. In contrast to previous reports in the moss *Physcomitrella Patens* (Kamisugi et al., 2006), we observed no concatenation of transgenes during homologous recombination. Taken together our results suggest that HR will be the method of choice for targeted gene disruption of for the knock-in of transgenes in *Ostreococcus*.

HR was observed at frequencies varying between 1 and 100% depending on the construct and the recipient stain. The length of homology was a key factor to determine the efficiency of gene targeting, but the mechanism of transgene selection had no effect. The GC content of the transgene was not important, as shown by the similar rates of recombination of the *KanMx* and *Nat1* sequences (40% and 60% GC, respectively*)* with the Wt gene.

The identification of HR events could be made even more effective by the use of a counter-selection marker to select against random insertion events. For example, the use of chlorate facilitated the selection of *NR* knock-out mutants in *Chlamydomonas* in spite of the

very low frequencies of HR in this green microalga (Sodeinde and Kindle, 1993). However, our attempts to use chlorate as a counter selection marker in *Ostreococcus* have failed, all chlorate resistant clones being false positives and able to grow on nitrate.

A memory of recombination events at the *nitrate reductase* locus?

To our surprise, gene integration occurred exclusively by HR when the native *NR* sequence was used to replace the disrupted *NR* sequence in *HR1KanMx* lines. Rates of HR were also high (65%) when a construct containing a *KanMx* selection marker was used to replacing the *Nat1* sequence in *HR1Nat* lines. This constrasted with the much lower rates of HR when transforming Wt cells with the *KanMx* disruption cassette. The restored *NR* locus resulting from the complementation of the *NR* knock out by the Wt gene also displayed low rates of HR.

We suggest that elevated rates of HR in HR1 *HR1KanMx* and *HR1Nat* lines result from the presence of insertions at the *NR* locus. This implies that *Ostreococcus* is somehow able to discriminate between "self" and foreign DNA. Whether such a mechanism exists also in other species remains an open question. There is a precedent in budding yeast, however, where insertion of the prokaryotic Tn3-beta lactamase into the genome also resulted in a hotspot for meiotic recombination (Stapleton and Petes, 1991). The genome of *O.tauri* has one of the highest gene densities known for a free living eukaryote, and contains very few repeated and transposon-like sequences (Derelle et al., 2006). This suggests that efficient mechanisms operate to remove foreign DNA from the genome. It is tempting to speculate that one such mechanism may be based on homologous recombination. This would require the pairing of homologous DNA sequences. *O. tauri* is haploid in culture, but pairing of homologous chromosomes may occur during mating. The comparisons of *O. tauri* strains support the existence of cryptic sex, although this remains to be demonstrated under laboratory conditions (Grimsley et al., 2010). Whether homologous recombination takes place during sexual reproduction or not, the mechanism by which DNA is recognized as foreign and marked as a recombination hotspot is unknown. We hypothesized that this may be mediated through changes in chromatin structure, because histone modifications such as H3K4Me can modulate the rate of recombination, and meiotic hotspots are usually associated with an open chromatin structure (Borde et al., 2009, Berchowitz and Hanlon, 2009). We did not observe any obvious correlation between the abundance of H3 trimethyl K4, H3 acetyl K9 or the nucleosome density at the *NR* locus, and the rate of HR in *Ostreococcus*, however other chromatin modifications such as DNA methylation may play a role (Maloisel and Rossignol,

1998). Our results indicate that recombination frequencies vary with chromosomal location, which may reflect different states of the chromatin. For example, while the rate of HR to replace the ferritin ORF with a selection marker was only 1%, it was 25% for the KI construct which was targeted 500 bp downstream. This suggests that the recombination rate is dependent of the locus and the chromatin state, which can vary along chromosomes.

Conclusion

For most model organisms like the plant *Arabidopsis thaliana*, large insertion collections of mutants are used to compensate for the lack of efficient gene targeting technologies. Our results indicate that, in *O. tauri*, gene targeting by homologous recombination can be used to knock-out specific genes, or to fuse a protein using an epitope tag or a reporter gene. The whole process of gene targeting, from transformation of the transgene to the identification of haploid knock-out lines by PCR, takes about three weeks. In the future, this technology could be used to introduce mutations at selected positions into the DNA. When combined with the use of an inducible promoter (Djouani-Tahri et al., 2011b), this should facilitate the controlled and inducible expression of recombinant proteins from specific loci. These tools promise a bright future to *Ostreococcus* as a “green yeast” for functional genomics, systems biology and biotechnological developments.

EXPERIMENTAL PROCEDURES

Algal culture, genetic transformation and biological tests

O. tauri 0TTH0595 strain was grown in flasks (Sarstedt) or white 96 wells microplates (Nunc, Perkin Elmer) under constant light at a light intensity of 20 µmol quanta cm^{-2} s^{-1}. Cells were grown in standard Keller medium, which contained natural seawater supplemented with trace metals and vitamins unless otherwise stated. Cell counting was performed by flow cytometry using a Cell Lab Quanta™ SC MPL – (Beckman Coulter). Cells were fixed in 0.25% glutaraldehyde for 20 min before flow cytometry analysis.

Genetic transformation was carried out by electroporation as previously described [11]. Stable transformant colonies were selected in semi-solid medium at 0.2% w/v agarose (low melting point agarose, Invitrogen) in Keller Medium supplemented with the appropriate antibiotic G418 at 1 mg/ml (calbiochem), or Clonat (nourseothricin) at 2 mg/ml (WERNER BioAgents Germany). For the *nitrate reductase* targeting experiments a Keller-based Artificial Sea Water (WERNER BioAgents Germany ASW) medium was used. This modified Keller medium contained 24.55 g/l NaCl, 0.75 g/l KCl, 4.07 g/l $MgCl_2$ $6H_2O$, 1.47 g/l $CaCl_2$,$2H_2O$, 6.04 g/l $MgSO_4 7H_2O$, 0.21 g/l $NaHCO_3$, 0.138 g/l NaH_2PO_4 and 0.75g/l $NaNO_3$. NR^{ko} were selected on this medium supplemented with 0.534 g/l NH_4Cl. In *NR* complementation experiments, $NaNO_3$ was the only source of nitrogen.

NR^{ko} transformants were identified by their ability to grow on ASW lacking ammonium in microplates and confirmed by PCR tests (see below). Disruption of *Nat1* or *KanMx* genes was identified by the inability to grow on G418 at 1 mg/ml, or on Clonat at 2 mg/ml. These tests were carried out with individual transformants grown in microplates.

Cloning strategy for gene targeting experiments

PCR Amplifications were performed on *O. tauri* genomic DNA using the Triple Master polymerase mix (Eppendorf). Primer sequences are given in Table S1. *Bgl*II and *Nco*I sites were added to the 5' and 3'ends of the 1102 bp *ferritin* PCR product to allow subsequent cloning. A sub-cloning step was performed in the pGEMT-easy vector (Promega). The *pH4::KanMx::Tef* selection cassette from the pOtluc vector was introduced into the coding sequence of *NR* and *ferritin* by blunt-end ligation into *Afe*I (AGC/GCT) or *Nru*I (TCG/CGA) sites, respectively. The same strategy was used to introduce pH4::clonat::Tef selection gene from the pOtox vector into the *NR* sequence. The *ferritin-luc* knock-in construct was

generated by cloning the full-length *ferritin* gene into the *Bgl*II-*Nco*I sites of the pOT-Luc vector, in frame with *luciferase*. A 1102 bp fragment corresponding to the 3' end of the *ferritin* gene was then ligated into the *Sma*I site of pOtluc. The resulting construct (5462bp) comprised the full length *ferritin* gene fused in frame with *luciferase*, upstream of the *KanMx* selection gene. Prior to transformation, plasmids were digested with appropriate restriction enzymes and purified onto "NucleoSpin® Gel and PCR Clean-up" kit (Macherey Nagel).

Molecular analysis of transformants

Ostreococcus Transformants were analyzed by PCR using transgene-specific primers (See able S1) and/or by Southern blot analysis. Genomic DNA was extracted using the DNAeasy Plant Minikit (Qiagen). For DNA blots, 1 microgram DNA was digested with appropriate enzymes, migrated in a 0.8% TAE agarose gel and transferred onto Hybond N+ membrane (Amersham) as previously described (Corellou et al., 2009). DNA probes were generated by PCR amplification using primers described in Table S1, except for the P3 probe corresponding to the *KanMx* sequence, which was excised from the pOtluc vector using *Hind*III and *Eco*RI. All probes were radiolabeled by random priming. Hybridization and washing of the membranes were performed as previously described (Corellou et al., 2009).

Chromatin immunoprecipitation (ChIP)

Cultures were grown in constant light until late log-phase. Cells were fixed by addition of formaldehyde to the medium to a concentration of 1% (v/v). Glycine was added after 10 minutes to a 125 mM concentration. After 5 minutes, cells were washed twice with ice-cold PBS. Cell pellets were frozen in liquid nitrogen then stored at -80^{o}C until extraction. In order to extract chromatin, cells were resuspended into extraction buffer (50 mM Tris-HCl pH 8, 10 mM EDTA, 1% SDS) containing a protease inhibitor cocktail (Roche) prior to sonicating three times 10 seconds at 50-second intervals using a Branson sonifier. The cell lysate was centrifuged at 10,00 rpm for 10 minutes and the supernatant containing the chromatin was frozen at -80oC. For ChIP analyses, 200 µl of chromatin were diluted to 2 ml using ChIP dilution buffer (167 mM NaCl, 16.7 mM Tris-HCl pH8, 1.2 mM EDTA, Triton X-100, 1 mM PMSF and protease inhibitors). After preclearing with protein A Dynabeads (Invitrogen), samples were incubated overnight at 4°C with either anti-H3 (1:200), anti H3-Acetyl K9 or anti-H3 trimethyl K4 antibodies (Abcam). The immuno-complexes were isolated by incubation with protein A Dynabeads for 2 h at 4°C. The beads were washed as described (Haring et al, 2007) with the addition of three extra high salt buffer washes. DNA to be

analysed by qPCR was eluted from the beads in the presence of 10% Chelex according to (Nelson et al, 2006). Real-time PCR was carried out on a LightCycler 1.5 (Roche Diagnostic) with LightCycler DNA Master SYBR Green I (Roche Molecular Biochemicals) Putative target loci in immunoprecipitated samples were amplified using specific primers (Table S1). Results were analysed using the comparative critical threshold ($\Delta\Delta C$T) method, quantified relative to the original input chromatin sample and presented as percent of input DNA.

Western Blot analysis.

Cells were harvested by centrifugation in conical bottles (10 000g, 4°C, 10min), after addition of pluronic (0.1%) to the medium. Pellet were frozen in liquid nitrogen and stored at – 80°C until extraction. Cells were ground in lysis buffer (100mM potassium phosphate pH 7.8, 1 mM EDTA, 1 mM DTT, 1% Triton® X-100, 10% glycerol) using a RNA Tissue lyser. Protein concentration was determined by the Bradford method (Sigma) and the same amount of protein was loaded in each well on a 10 %SDS-polyacrylamide denaturing gel 4X Laemmli buffer. Western blot analysis was performed as following: the gel was liquid-transferred onto a Nylon membrane (PVDF, Amersham Life Science, Buckingamshire, UK). The membranes were blocked in Tris Buffer Saline (TBS) containing 5 % milk powder antibody for one hour and then incubated with an anti-luciferase antibody (sc-74548, Santa Cruz Biotechnology, Inc) at a 1/2 000 dilution The membranes were washed 3 to 6 times in TBS containing 0.1% Tween 20 and the bound antibody was detected with a goat anti mouse antibody (sc-2005). Immunodetection was performed using the ECL+ reagent (Amersham Life Science). Recombinant luciferase from *Photinus pyralis* (Sc-32896) was used as a positive control.

Acknowledgements

This work was supported by ASSEMBLE EU Project to FYB and IC and ANR Phytoiron to EL and FYB. Thanks to Charles White for helpful discussions and advices

Construct (Recipient Wt)	Transformants				
	Selection	Growth on NH_4^+ (HR+RI)	No Growth on $N0_3^-$ (%)	HR lines confirmed by PCR analyses (Number of tested lines)	Name of HR lines
KanMx-as	G418	425	8* (~2%)	8 (20)	HR1 *KanMx-as*
KanMx-s	G418	107	1* (~1%)	1 (20)	HR1 *KanMx-s*

Table 1. Effect of construct orientation on the frequency of HR at the *NR* locus.
* lines were all analyzed by PCR

Construct	Homology Length (kbp)		Recipient strain	Selection	Transformants				
	5’	3’			$N0_3^-$ growth (%)	G418 growth (%)	CloNat growth (%)	PCR HR lines (% HR/RI)	Name of HR lines
Nit	1.9	2.5	*HR1 KanMx-s*	$N0_3^-$	219 (100%)	0	N/A	20 (20) (100%)	*HR2Nit KanMx-s*
Nit	1.9	2.5	*HR1 KanMx-as*	$N0_3^-$	54 (100%)	0	N/A	54 (54) (100%)	*HR2Nit KanMx-as*
pH4Nat	0.5	0.25	*HR1 KanMx-s*	CloNat	N/A	122	4 (3%)	4 (122) (3%)	*H1RNat*
KanMx-s	1.9	2.5	*HR1Nat*	G418	N/A	60	21 (35%)	39 (60) (65%)	*HR2 KanMx-s*
KanMx-s	1.9	2.5	*HRNit1*	G418	0 (0%)	192	N/A	0 (192) (0%)	*HR3 KanMx-s*

Table 2. Gene replacements at the *NR* locus. All transformants were analyzed by PCR

FIGURE LEGENDS

Figure 1: Strategy for the targeted disruption of the *nitrate reductase* (*NR*) gene in *O. tauri*. (a) Physical map of the *NR* locus and of the constructs used in the study. Homologous sequences are highlighted in grey and selection genes in black. The *pH4:Nat1* construct shares promoter and terminator sequences with the *pH4:KanMx* sequence of *KanMx-as* and *KanMx-s* constructs. **(b)** Identification of a putative *NR* knock-out line. The *KanMx-as* construct was electroporated into *O. tauri* cells. Transformants resistant to G418 were selected in ASW agarose medium containing NH_4^+. Their growth was further tested in liquid ASW medium containing $N0_3^-$ as the sole source of nitrogen. Most of the clones also grew on $N0_3^-$ (red arrow). However, those that grew on NH_4^+ but failed to grow on $N0_3^-$ identified putative *NR* disruptants (green arrow).

Figure 2: Targeted disruption of the *NR* gene by homologous recombination using antisense *KanMx* constructs. (a) Expected physical maps of homologous recombinants (*HR1KanMx-as)* and random insertion lines (*RI1KanMx-as).* The Wt *NR* locus is expected to remain intact if insertion takes place at a random genomic location. **(b)** Analysis of *HR1KanMx-as* lines. Left: PCR analyses using either internal *NR* (F1,R1) or external and *KanMx* (F2,R2) primers. Right: Southern Blot analysis. DNA was digested with *Kpn*I and hybridized to either *NR* or *KanMx* specific probes P1 and P2, respectively. All of the clones that failed to grow on nitrate had patterns of amplification and hybridization consistent with *NR* disruption by homologous recombination. **(c)** Summary of the *NR* targeting experiments, showing the history of each of the lines. Lines marked with stars were used for chromatin immunoprecipitation experiments in Figure 5.

Figure 3: High frequency transgene removal from the NR locus by HR. *HR1KanMx-s* or *-as* cell lines were transformed using a Wt *NR* sequence fragment and selected on nitrate-ASW. **(a)** Expected physical maps of homologous recombinants (*HR2Nit)* and random insertion lines (*RINit).* HR between the Wt transgene and the disrupted locus in the parental cell lines should lead to restoration of the Wt locus. However, RI of the *NR* sequence should introduce an additional copy of the *NR* locus elsewhere in the genome (indicated by Chr?). (b) analysis of transformants. Left: PCR analysis using the F1 and R1 primers. All transformants that grew on nitrate gave 0.6 kbp PCR bands typical of the Wt *NR* locus. Right: Southern

Blot analysis. Genomic DNA from transformants, from the HR1 recipient and from a Wt cell line was digested with *Hind*III and *Pst*I and hybridized to the *NR* probe P3. The line marked with a star was used for chromatin immunoprecipitation experiments in Figure 5.

Figure 4: Effect of the length of homologous sequences on the efficiency of gene targeting. A cell line resistant to CloNat (*HR2Nat*) was transformed using constructs containing either 2.5, 1, or 0.5 kbp of sequence homologous to *NR* on either side of the *KanMx-s* resistance cassette. The percentage of transgene insertion by HR is plotted on the X axis.

Figure 5: Chromatin remodeling during successive homologous recombination events. (a) Diagram of the *NR* locus, indicating the regions tested. **(b)** Top row: changes in nucleosome density were tested by ChIP using antibodies to histone H3. Middle and bottom rows: changes in chromatin opening and closing marks (histone H3 acetyl K9 and histone H3 trimethyl K4, respectively), also determined by ChIP. Each bar represents averaged data from three independent wild-type cultures or HR lines. Error bars indicate standard deviations.

Figure 6: Targeted knock-out and knock-in of the luciferase reporter at the *ferritin* locus. (a) knock-out of the *ferritin* gene. Wt cells were transformed using a *ferritin* sequence fragment disrupted by the *KanMx* selection marker. Transformants were identified by selection on G418. Homologous recombination was confirmed by the obtention of a 0.9 kbp PCR product using the primers FFe and RFo, and of a 2.5 kbp PCR product using the primers FFe and RFe. RIFe indicates *Ferritin* random insertion lines and *HRFe,* homologous insertion lines. **(b)** In frame knock-in of the luciferase reporter. A construct in which the luciferase reporter gene was inserted in frame downstream of the *ferritin* ORF was electroporated into *O. tauri* cells. Knock-in lines (*HRFlu*) were identified by PCR using either a combination of selection marker FH4 and external primers RFi, or using the *ferritin* specific primers FFo and RRFo. *RIFlu* indicates a random insertion of the *ferritin-luc* construct. Bottom: Western Blot analysis using an anti-luc (α-luc) antibody detected a protein at 85 kda in *HRFlu* and *RiFlu* lines. *Luc* indicates recombinant luciferase protein (65 kda), expressed in *O. tauri* under control of the High affinity phosphate transporter.

REFERENCES

Berchowitz, L. and Hanlon, S. (2009). A positive but complex association between meiotic double-strand break hotspots and open chromatin in Saccharomyces cerevisiae. *Genome Research*,,2245–2257.

Borde, V., Robine, N., Lin, W., Bonfils, S., Géli, V., and Nicolas, A. (2009). Histone H3 lysine 4 trimethylation marks meiotic recombination initiation sites. *The EMBO journal*, **28**,99–111.

Corellou, F., Schwartz, C., Motta, J.-P., Djouani-Tahri, E.B., Sanchez, F., and Bouget, F.-Y. (2009). Clocks in the green lineage: comparative functional analysis of the circadian architecture of the picoeukaryote *Ostreococcus. The Plant cell*, **21**,3436–49.

Cummings, W.J., Yabuki, M., Ordinario, E.C., Bednarski, D.W., Quay, S., and Maizels, N. (2007). Chromatin structure regulates gene conversion. *PLoS biology*, **5**,e246.

Dawson, H., Burlingame, R., and Cannons, A. (1997). Stable Transformation of Chlorella: Rescue of Nitrate Reductase-Deficient Mutants with the Nitrate Reductase Gene. *Current microbiology*, **35**,356–62.

Derelle, E., Ferraz, C., Rombauts, S., Rouzé, P., Worden, A.Z., Robbens, S., Partensky, F., Degroeve, S., Echeynié, S., Cooke, R., Saeys, Y., Wuyts, J., Jabbari, K., Bowler, C., Panaud, O., Piégu, B., Ball, S.G., Ral, J.-P., Bouget, F.-Y., Piganeau, G., et al. (2006). Genome analysis of the smallest free-living eukaryote Ostreococcus tauri unveils many unique features. *Proceedings of the National Academy of Sciences of the United States of America*, **103**,11647–52.

Djouani-Tahri, E.-B., Christie, J.M., Sanchez-Ferandin, S., Sanchez, F., Bouget, F.-Y., and Corellou, F. (2011a). A eukaryotic LOV-histidine kinase with circadian clock function in the picoalga Ostreococcus. *The Plant journal*, **65**,578–88.

Djouani-Tahri, E.B., Sanchez, F., Lozano, J.-C., and Bouget, F.-Y. (2011b). A phosphate-regulated promoter for fine-tuned and reversible overexpression in Ostreococcus: application to circadian clock functional analysis. *PloS one*, **6**,e28471.

Gan, L., Ladinsky, M., and Jensen, G. (2011). Organization of the smallest eukaryotic spindle. *Current Biology*, **21**,1578–1583.

Grimsley, N., Péquin, B., Bachy, C., Moreau, H., and Piganeau, G. (2010). Cryptic sex in the smallest eukaryotic marine green alga. *Molecular biology and evolution*, **27**,47–54.

Heijde, M., Zabulon, G., Corellou, F., Ishikawa, T., Brazard, J., Usman, A., Sanchez, F., Plaza, P., Martin, M., Falciatore, A., Todo, T., Bouget, F.-Y., and Bowler, C. (2010). Characterization of two members of the cryptochrome/photolyase family from Ostreococcus tauri provides insights into the origin and evolution of cryptochromes. *Plant, cell & environment*, **33**,1614–26.

Heyer, W.-D., Ehmsen, K.T., and Liu, J. (2010). Regulation of homologous recombination in eukaryotes. *Annual review of genetics*, **44**,113–39.

Kamisugi, Y., Schlink, K., Rensing, S. a, Schween, G., Von Stackelberg, M., Cuming, A.C., Reski, R., and Cove, D.J. (2006). The mechanism of gene targeting in Physcomitrella patens: homologous recombination, concatenation and multiple integration. *Nucleic acids research*, **34**,6205–14.

Keeney, S., Giroux, C.N., and Kleckner, N. (1997). Meiosis-specific DNA double-strand breaks are catalyzed by Spo11, a member of a widely conserved protein family. *Cell*, **88**,375–84.

Kilian, O., Benemann, C.S.E., Niyogi, K.K., and Vick, B. (2011). High-efficiency homologous recombination in the oil-producing alga Nannochloropsis sp. *Proceedings of the National Academy of Sciences of the United States of America*, **108**,21265–9.

Kotian, S., Liyanarachchi, S., Zelent, A., and Parvin, J.D. (2011). Histone deacetylases 9 and 10 are required for homologous recombination. *The Journal of biological chemistry*, **286**,7722–6.

Maloisel, L. and Rossignol, J.L. (1998). Suppression of crossing-over by DNA methylation in Ascobolus. *Genes & development*, **12**,1381–9.

Minoda, A., Sakagami, R., Yagisawa, F., Kuroiwa, T., and Tanaka, K. (2004). Improvement of culture conditions and evidence for nuclear transformation by homologous recombination in a red alga, Cyanidioschyzon merolae 10D. *Plant & cell physiology*, **45**,667–71.

Monnier, A., Liverani, S., Bouvet, R., Jesson, B., Smith, J.Q., Mosser, J., Corellou, F., and Bouget, F.-Y. (2010). Orchestrated transcription of biological processes in the marine picoeukaryote Ostreococcus exposed to light/dark cycles. *BMC genomics*, **11**,192.

Moulager, M., Corellou, F., Vergé, V., Escande, M.-L., and Bouget, F.-Y. (2010). Integration of light signals by the retinoblastoma pathway in the control of S phase entry in the picophytoplanktonic cell Ostreococcus. *PLoS genetics*, **6**,e1000957.

O'Neill, J.S., Van Ooijen, G., Dixon, L.E., Troein, C., Corellou, F., Bouget, F.-Y., Reddy, A.B., and Millar, A.J. (2011). Circadian rhythms persist without transcription in a eukaryote. *Nature*, **469**,554–8.

Pfeuty, B., Thommen, Q., Corellou, F., Djouani-Tahri, E.B., Bouget, F.-Y., and Lefranc, M. (2012). Circadian clocks in changing weather and seasons: lessons from the picoalga Ostreococcus tauri. *BioEssays : news and reviews in molecular, cellular and developmental biology*, **34**,781–90.

Schaefer, D.G. and Zryd, J.-P. (1997). Efficient Gene targeting in the moss Physcomirella patens. *Plant Journal*, **11**,1195–1206.

Shinohara, a, Ogawa, H., and Ogawa, T. (1992). Rad51 protein involved in repair and recombination in S. cerevisiae is a RecA-like protein. *Cell*, **69**,457–70.

Sodeinde, O.A. and Kindle, K.L. (1993). Homologous recombination in the nuclear genome of. *Proceedings of the National Academy of Sciences of the United States of America*, **90**,9199–9203.

Stapleton, A. and Petes, T.D. (1991). The Tn3 beta-lactamase gene acts as a hotspot for meiotic recombination in yeast. *Genetics*, **2**,39–51.

Zorin, B., Lu, Y., Sizova, I., and Hegemann, P. (2009). Nuclear gene targeting in Chlamydomonas as exemplified by disruption of the PHOT gene. *Gene*, **432**,91–6.

SUPPLEMENTARY FIGURES LEGENDS

Figure S1: Targeted disruption of the *NR* gene by homologous recombination using sense *KanMx* constructs. (a) Expected physical maps of homologous recombinants (*HR1KanMx-s)* and random insertion lines (*RI1KanMx-s).* The Wt *NR* locus is expected to remain intact if insertion takes place at a random genomic location. **(b)** Analysis of *HR1KanMx-as* lines. Left: PCR analyses using either external and *KanMx* (F3, R2) or internal *NR* (F1, R1) primers. Right: Southern Blot analysis. DNA was digested with *Kpn*I and hybridized to *NR* specific probe P1.

Figure S2: Selection marker replacements by homologous recombination. **(a)** Generation of a CloNat resistant *HR1Nat* line by homologous recombination. A *HR1KanMx-s* line was transformed with the *pH4:Nat1* cassette which shares homology over the promoter and terminator regions of the *KanMx* cassette. Top row: Expected physical maps of homologous recombinants (*HR1Nat)* and random insertion lines (*RI1Nat).* Bottom row: PCR analysis of transformants using promoter Fp and terminator Rt specific primers. The four *HR1Nat* lines, which became sensitive to G418 had patterns of amplification consistent with homologous replacement of the *KanMx* sequence by *Nat1*. **(b)** Homologous replacement of *Nat1by KanMx* sequence. A HR1Nat line generated in (a) was transformed with the *KanMx-s* construct. Top row: expected physical maps of homologous (*HR2KanMx-s)* and random insertion lines (*RI2KanMx-s).* Bottom row: PCR analysis of transformants using promoter Fp and terminator Rt specific primers. The *HR2KanMx-s* lines, which became sensitive to CloNat had patterns of amplifications consistent with homologous replacement of the *Nat1* by *KanMx* sequence.

Figure S3: Targeting of the *NR* restored line. A *HR2Nit* (*KanMx-s* parental line) restored line was targeted by the *KanMx-s* construct (see Figure 1). Transformants were selected on NH_4^+ -ASW containing G418. Top row: expected physical maps of homologous recombinants (*HR3KanMx-s)* and random insertion (*RI3KanMx-s)* lines. Bottom row: PCR analysis of transformants using (F1, R1) *NR* specific primers. All transformants displayed the 0.6 kbp *NR* Wt band consistent with a random insertion of the *KanMx-s sequence.*

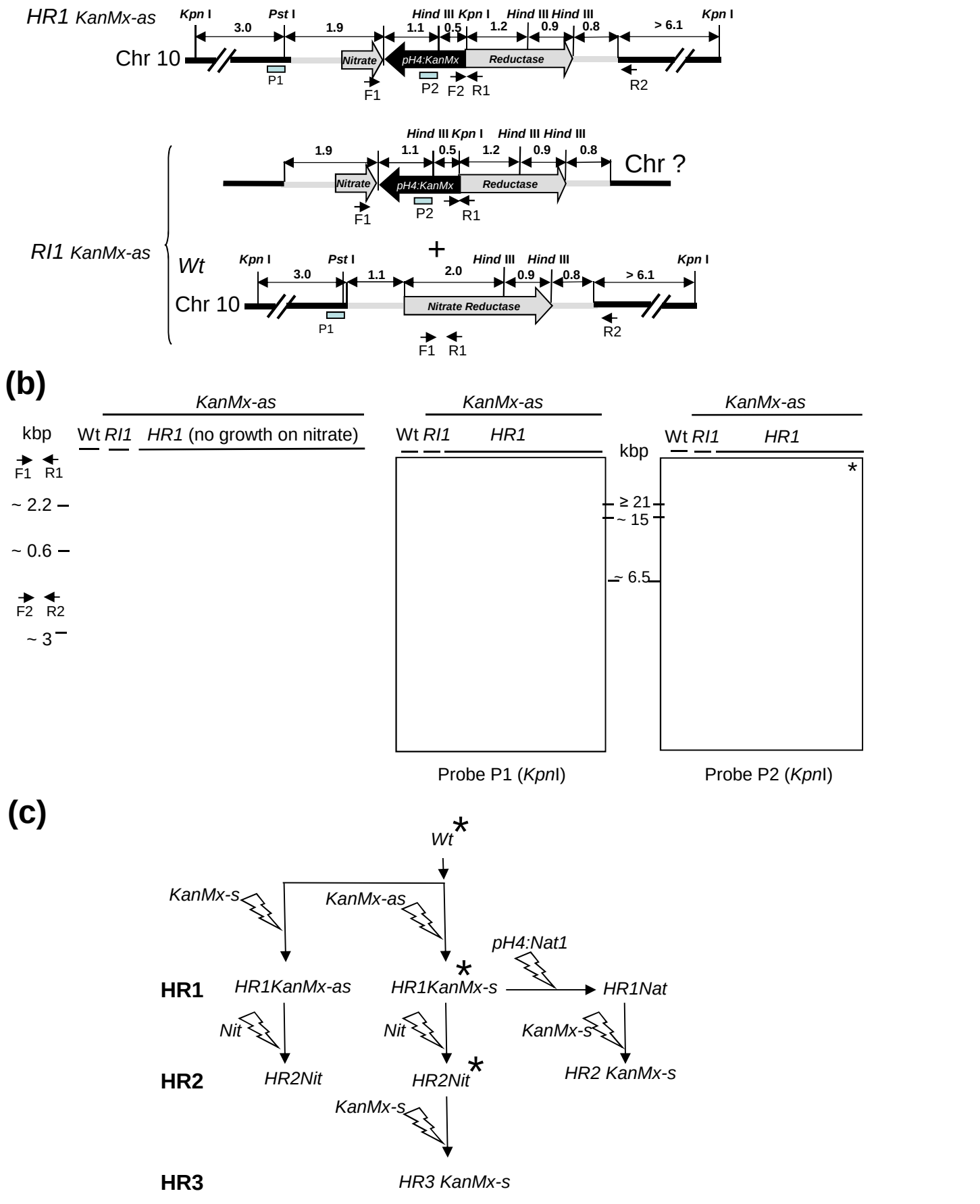
(a)
Transformants resistant to G418
HR1 KanMx-as
Chr 10
Kpn I
Pst I
Hind III Kpn I
Hind III Hind III
Kpn I
3.0
1.9
1.1
0.5
1.2
0.9
0.8
> 6.1
Nitrate
pH4:KanMx
Reductase
P1
F1
P2
F2
R1
R2
RI1 KanMx-as
Chr ?
Wt
Chr 10
2.0
Nitrate Reductase
(b)
KanMx-as
kbp
Wt
RI1
HR1 (no growth on nitrate)
HR1
~ 2.2
~ 0.6
~ 3
≥ 21
~ 15
~ 6.5
Probe P1 (KpnI)
Probe P2 (KpnI)
(c)
Wt
KanMx-s
KanMx-as
pH4:Nat1
HR1
HR1KanMx-as
HR1KanMx-s
HR1Nat
Nit
KanMx-s
HR2
HR2Nit
HR2 KanMx-s
HR3
HR3 KanMx-s

Figure 3

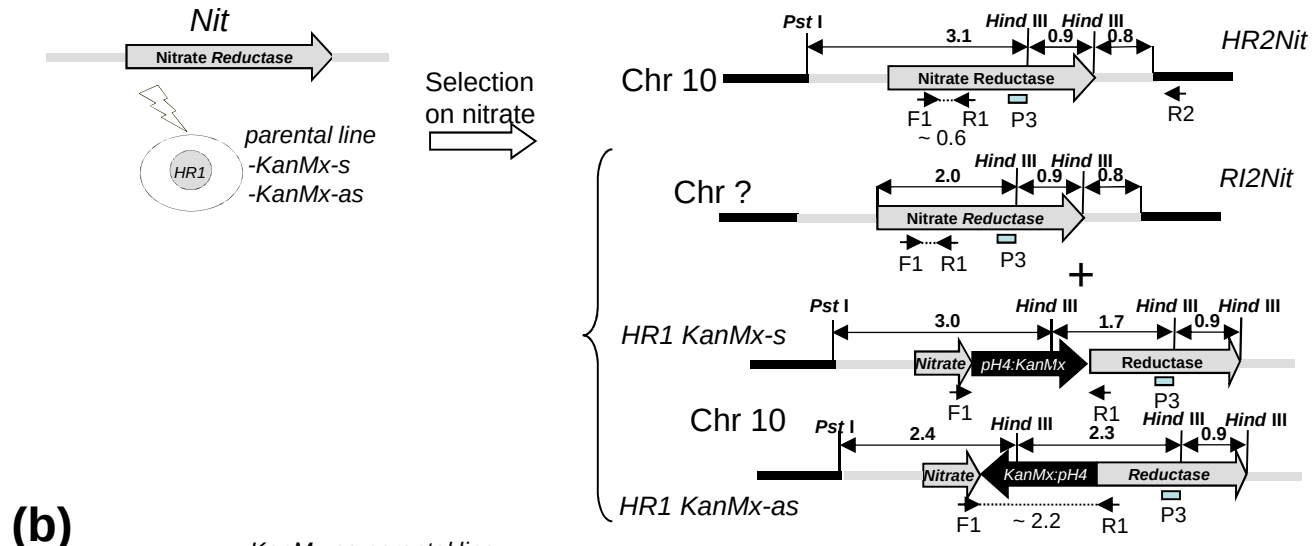
(a)
Nit
Nitrate Reductase
HR1
parental line
-KanMx-s
-KanMx-as
Selection
on nitrate
Chr 10
Pst I
Hind III
Hind III
3.1
0.9
0.8
HR2Nit
Nitrate Reductase
F1
R1
P3
~ 0.6
R2
Chr ?
2.0
0.9
0.8
RI2Nit
Nitrate Reductase
F1
R1
P3
+
HR1 KanMx-s
Pst I
Hind III
Hind III
Hind III
3.0
1.7
0.9
Nitrate
pH4:KanMx
Reductase
F1
R1
P3
Chr 10
Pst I
Hind III
Hind III
Hind III
2.4
2.3
0.9
Nitrate
KanMx:pH4
Reductase
HR1 KanMx-as
F1
~ 2.2
R1
P3

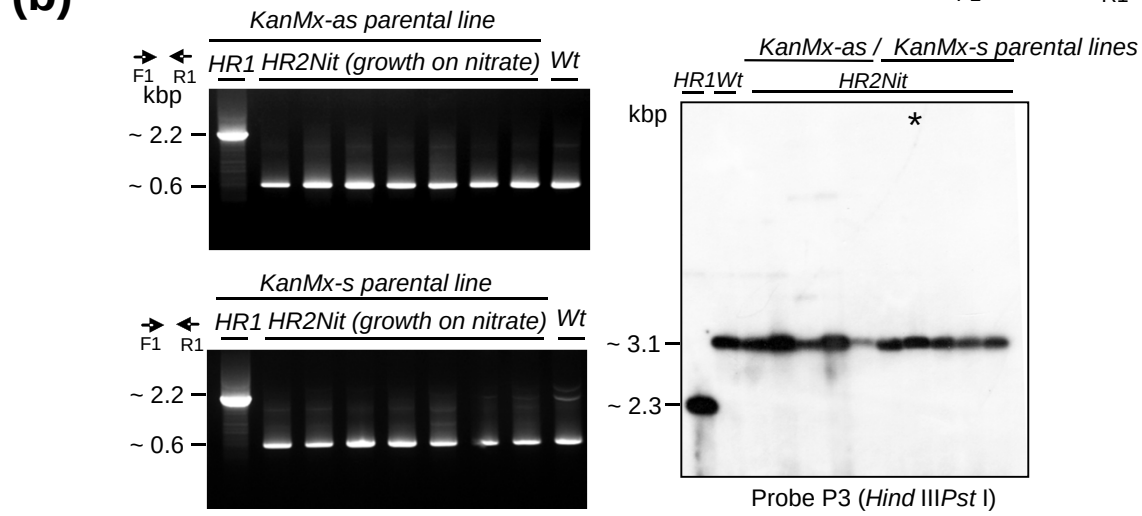
(b)
KanMx-as parental line
F1
R1
HR1
HR2Nit (growth on nitrate)
Wt
kbp
~ 2.2
~ 0.6
KanMx-s parental line
F1
R1
HR1
HR2Nit (growth on nitrate)
Wt
~ 2.2
~ 0.6
KanMx-as / KanMx-s parental lines
HR1Wt
HR2Nit
kbp
*
~ 3.1
~ 2.3
Probe P3 (Hind IIIPst I)

Figure 4

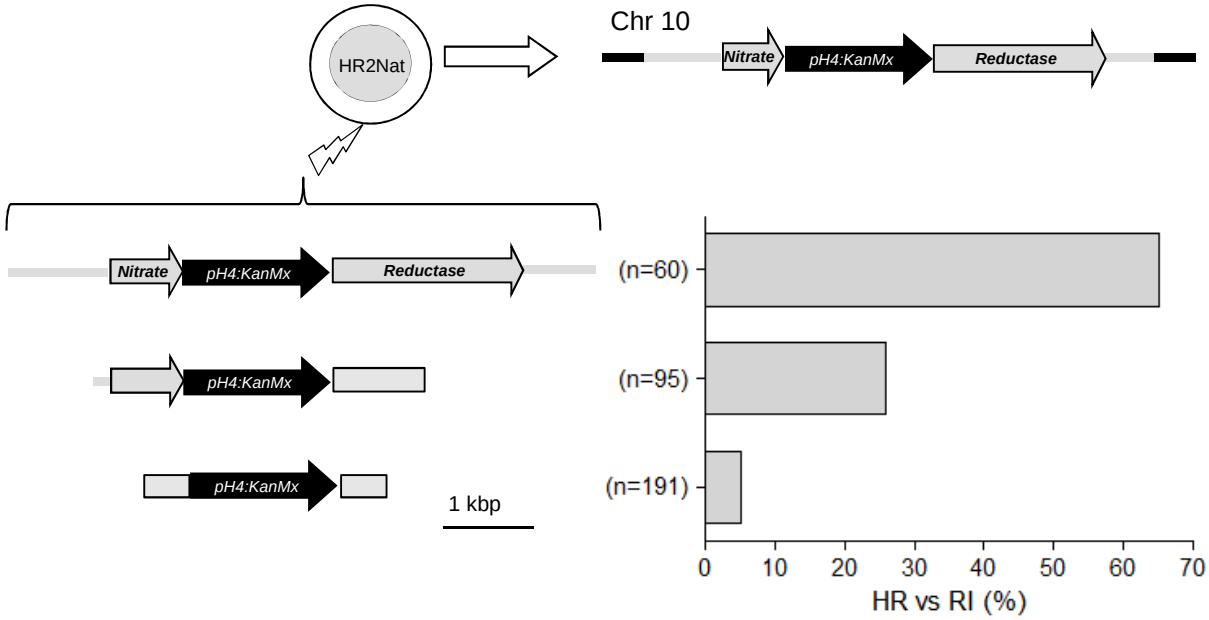
HR2Nat
Chr 10
Nitrate
pH4:KanMx
Reductase
Nitrate
pH4:KanMx
Reductase
pH4:KanMx
pH4:KanMx
1 kbp
(n=60)
(n=95)
(n=191)
0
10
20
30
40
50
60
70
HR vs RI (%)

Figure 5

(a)

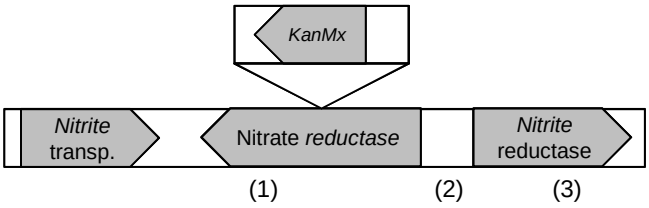
KanMx
Nitrite transp.
Nitrate reductase
Nitrite reductase
(1)
(2)
(3)

(b)

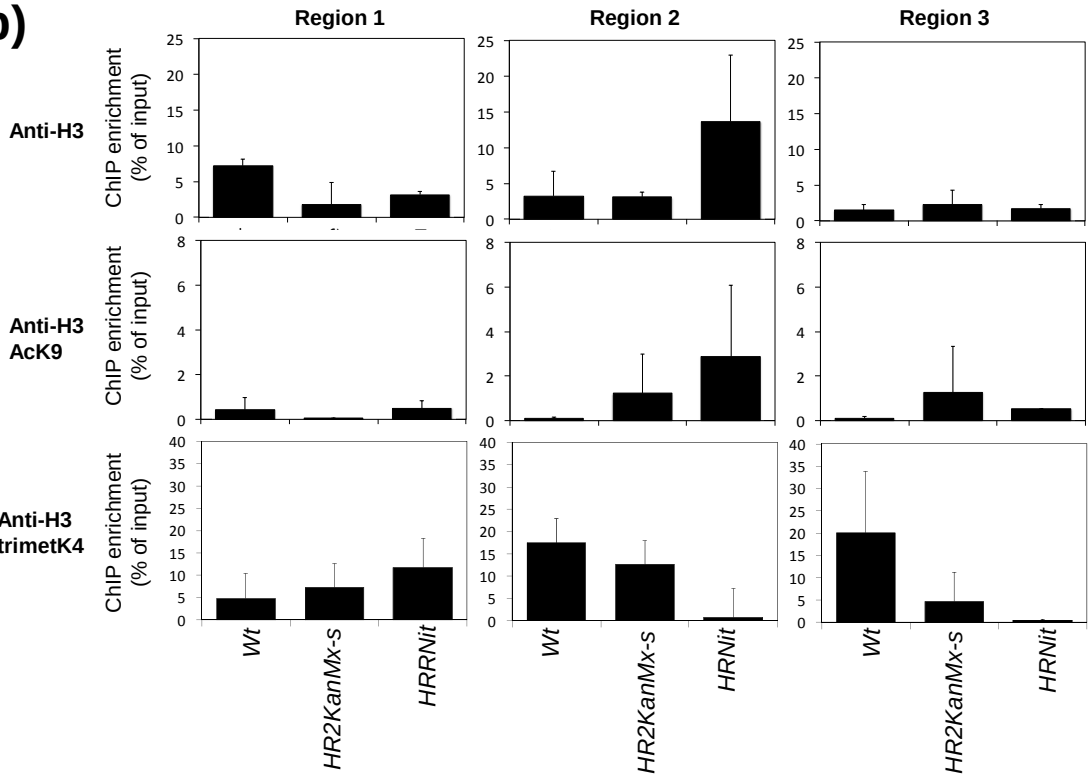
Region 1
Region 2
Region 3
Anti-H3
Anti-H3 AcK9
Anti-H3 trimetK4
ChIP enrichment (% of input)
Wt
HR2KanMx-s
HRRNit
HRNit

Figure 6

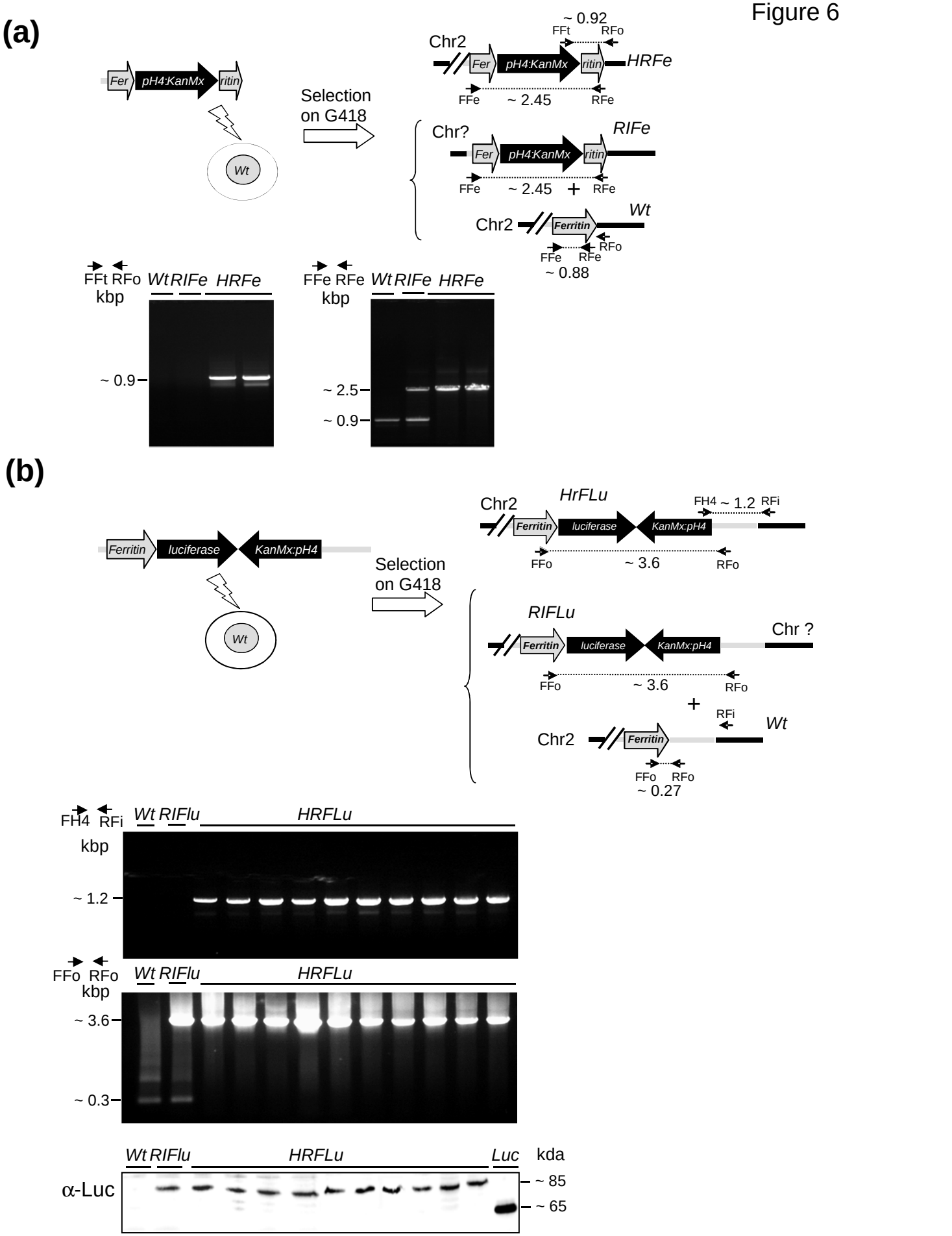
(a)
Fer
pH4:KanMx
ritin
Wt
Selection
on G418
Chr2
~ 0.92
FFt
RFo
HRFe
FFe
~ 2.45
RFe
Chr?
RIFe
+
Wt
Ferritin
~ 0.88
FFt RFo
kbp
Wt RIFe HRFe
~ 0.9
FFe RFe
~ 2.5
~ 0.9
(b)
Ferritin
luciferase
KanMx:pH4
HrFLu
FH4 ~ 1.2 RFi
FFo
~ 3.6
RFo
RIFLu
Chr ?
RFi
FH4 RFi
Wt RIFlu HRFLu
~ 1.2
FFo RFo
~ 3.6
~ 0.3
Luc
kda
α-Luc
~ 85
~ 65

Figure S1

(a)

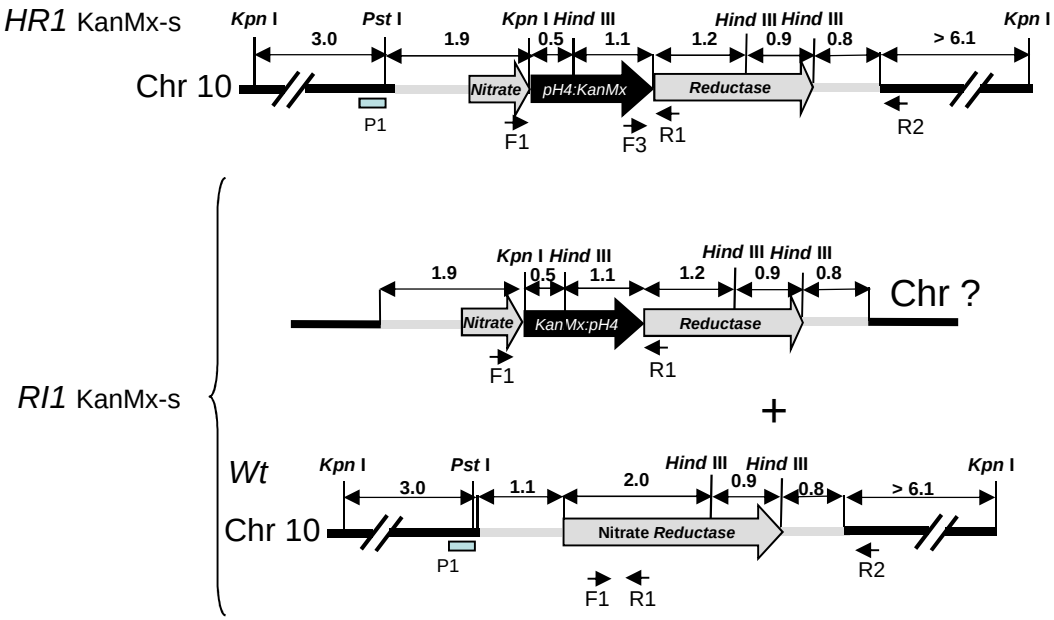
HR1 KanMx-s
Kpn I
Pst I
Kpn I Hind III
Hind III Hind III
Kpn I
3.0
1.9
0.5
1.1
1.2
0.9
0.8
> 6.1
Chr 10
Nitrate
pH4:KanMx
Reductase
P1
F1
F3
R1
R2
RI1 KanMx-s
Kpn I Hind III
Hind III Hind III
1.9
0.5
1.1
1.2
0.9
0.8
Chr ?
Nitrate
KanVx:pH4
Reductase
F1
R1
+
Wt
Kpn I
Pst I
Hind III
Hind III
Kpn I
3.0
1.1
2.0
0.9
0.8
> 6.1
Chr 10
Nitrate Reductase
P1
F1
R1
R2

(b)

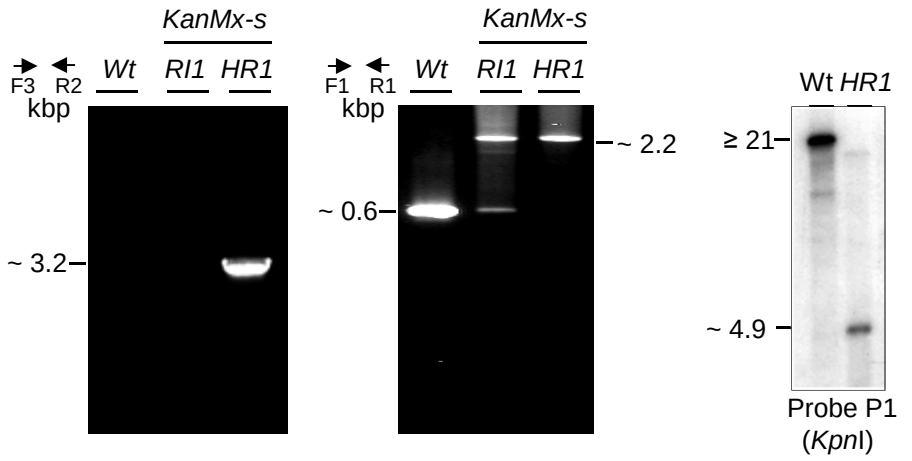
KanMx-s
F3
R2
Wt
RI1
HR1
kbp
~ 3.2
KanMx-s
F1
R1
Wt
RI1
HR1
kbp
~ 2.2
~ 0.6
Wt HR1
≥ 21
~ 4.9
Probe P1
(KpnI)

Figure S2

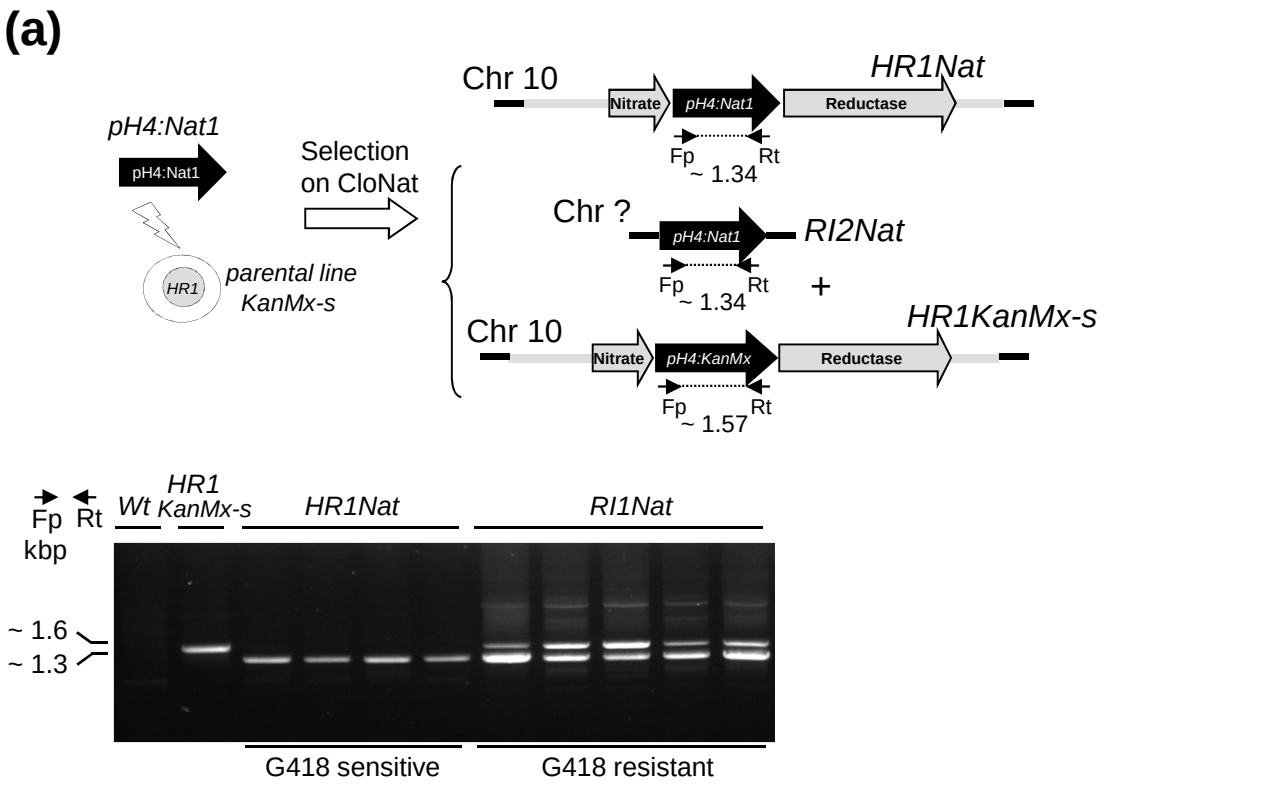
(a)
pH4:Nat1
pH4:Nat1
HR1
parental line
KanMx-s
Selection
on CloNat
Chr 10
HR1Nat
Nitrate
pH4:Nat1
Reductase
Fp
Rt
~ 1.34
Chr ?
RI2Nat
+
HR1KanMx-s
pH4:KanMx
~ 1.57
Fp Rt
kbp
Wt
HR1
KanMx-s
HR1Nat
RI1Nat
~ 1.6
~ 1.3
G418 sensitive
G418 resistant

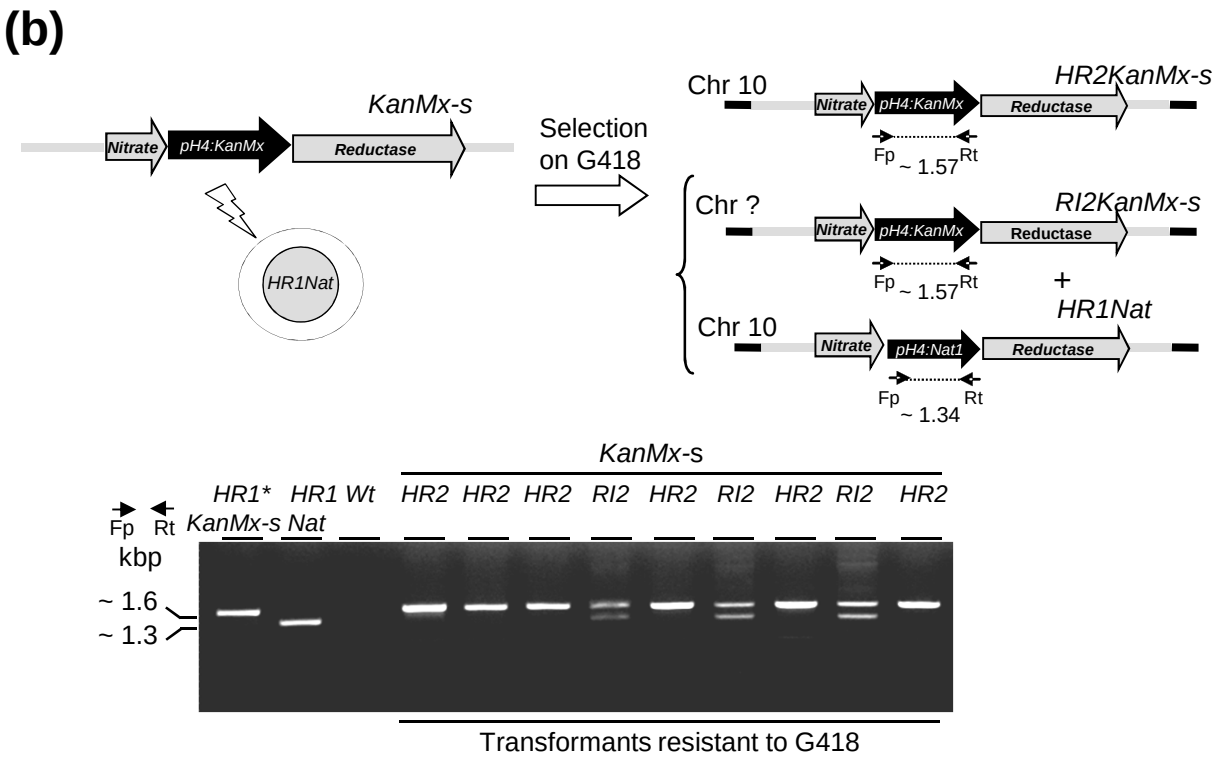
(b)
KanMx-s
Nitrate
pH4:KanMx
Reductase
HR1Nat
Selection
on G418
Chr 10
HR2KanMx-s
~ 1.57
Chr ?
RI2KanMx-s
+
HR1Nat
pH4:Nat1
~ 1.34
Fp Rt
kbp
HR1*
HR1 Wt
KanMx-s Nat
HR2
RI2
~ 1.6
~ 1.3
Transformants resistant to G418

Figure S3

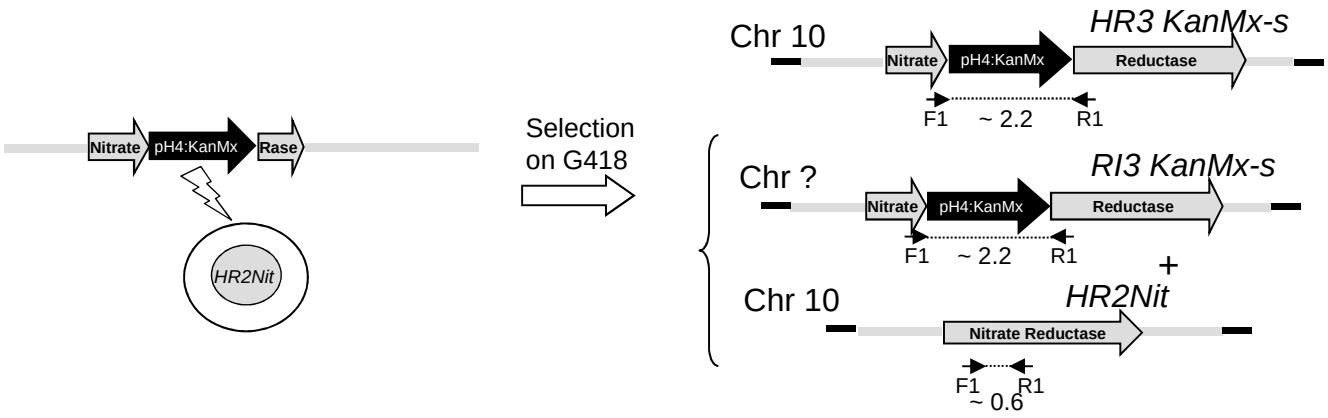
Nitrate
pH4:KanMx
Rase
HR2Nit
Selection
on G418
Chr 10
HR3 KanMx-s
Nitrate
pH4:KanMx
Reductase
F1
~ 2.2
R1
Chr ?
RI3 KanMx-s
Nitrate
pH4:KanMx
Reductase
F1
~ 2.2
R1
+
Chr 10
HR2Nit
Nitrate Reductase
F1
R1
~ 0.6

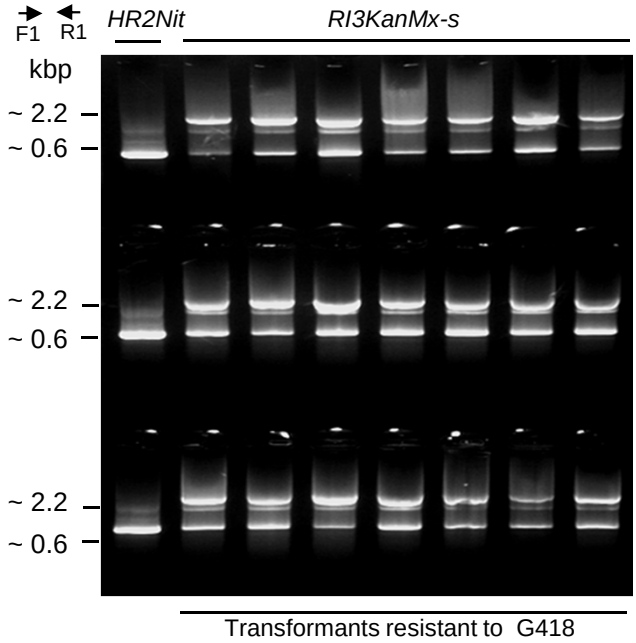
F1
R1
HR2Nit
RI3KanMx-s
kbp
~ 2.2
~ 0.6
~ 2.2
~ 0.6
~ 2.2
~ 0.6
Transformants resistant to G418